Journal of Alloys and Compounds 507 (2010) 178–183

Contents lists available at ScienceDirect

Journal of Alloys and Compounds

journal homepage: www.elsevier.com/locate/jallcom

Effect of hot rolling on the microstructure and mechanical properties of Mg–5Al–0.3Mn–2Nd alloy

Jianli Wang[a,b,*], Hanwu Dong[b,c], Lidong Wang[b], Yaoming Wu[b], Limin Wang[b]

[a] School of Materials and Chemical Engineering, Xi'an Technological University, Xi'an 710032, China
[b] State Key Laboratory of Rare Earth Resource Utilization, Changchun Institute of Applied Chemistry, Chinese Academy of Sciences, Changchun 130022, China
[c] Graduate University of Chinese Academy of Sciences, Beijing 100049, China

ARTICLE INFO

Article history:
Received 4 March 2009
Received in revised form 16 July 2010
Accepted 21 July 2010
Available online 30 July 2010

Keywords:
Mg–Al–Mn–Nd alloy
Hot rolling
Microstructures
Mechanical properties

ABSTRACT

Mg–5Al–0.3Mn–2Nd alloy was prepared by metal mould casting. The as-cast ingot was homogenized, and then hot-rolled with total thickness reduction of 63%. Further annealing treatment was carried out on the hot-rolled sample. Microstructure and mechanical properties of the studied alloy in as-cast, hot-rolled and annealed states were investigated. Results showed that main phases of the as-cast sample were composed of α-Mg, Al_2Nd, $Mg_{17}Al_{12}$ and $Al_{11}Nd_3$. While for the hot-rolled and annealed samples, no $Mg_{17}Al_{12}$ phase was detected. Average grain size of the as-cast sample was about 90 μm. After hot rolling, average grain size was greatly refined to about 20 μm. Furthermore, the long acicular $Al_{11}Nd_3$ phase broke into many small sections. Tensile test results showed that ultimate tensile strength and yield strength of the hot-rolled sample were 340 MPa and 240 MPa, respectively. Compared with those of the as-cast sample, they were enhanced by 47.8% and 269% correspondingly. However, elongation greatly decreased to 9%. Through annealing treatment, elongation recovered to more than 24% again.

© 2010 Elsevier B.V. All rights reserved.

1. Introduction

Magnesium alloys have gained extended application because of their unique advantages including low density, high specific strength and stiffness, superior damping capacity, good electromagnetic shielding characteristics and excellent machinability. Mg–Al based alloys like AZ91, AM60 and AM50 are widely used in automotive industry to fabricate various parts, owing to their superior die cast ability and good balance of strength, ductility and corrosion resistance. However, applications of these alloys are limited to temperatures below 120 °C because of their poor mechanical properties at elevated temperatures caused by discontinuous precipitation of $Mg_{17}Al_{12}$ phase from the supersaturated α-Mg solid solution at high temperatures and coarsening of $Mg_{17}Al_{12}$ phase in the interdendritic eutectic region [1–3]. Rare earth elements are often added to improve the mechanical properties of Mg–Al based alloys since they can suppress the formation of $Mg_{17}Al_{12}$ phase. And up to now, a series of Mg–Al–RE (RE = mischmetal) based casting alloys such as AE42 (Mg–4Al–2RE) [4] and AE44 (Mg–4Al–4RE) [5] alloys have been developed.

It is known that mechanical properties of polycrystals at room temperature can also be enhanced through grain refinement, as illustrated by the Hall–Petch equation [6]: $\sigma_y = \sigma_0 + k_y d^{-1/2}$, where σ_y is yield strength, σ_0 is yield strength of a single crystal, k_y is a constant and d is average grain size. The value of k_y increases with increasing Taylor factor [7] which generally depends on the number of slip systems. The fewer the slip systems, the larger the Taylor factor. It is known that the number of slip systems for the hexagonal closed packed (hcp) metals are much fewer than those of the face centered cubic (fcc) and body centered cubic (bcc) metals. Thus, larger Taylor factor could be obtained for hcp metals than for fcc and bcc metals. In other word, the effect of grain size on strength is stronger for hcp metals. This suggests that high strength could be obtained in fine-grained Mg-based materials. Based on this point, great efforts have been devoted to develop methods that could refine the grain size of Mg alloys. These methods reviewed by Lee et al. [8] include superheating, $FeCl_3$ addition, carbon additions, melt agitation, rapid solidification and alloying with elements such as Zr, Sr and Ti. However, a universally reliable grain refiner system for Mg–Al system alloys is still not established because of high cost and air pollution issues. Recently, thermo-mechanical treatments such as hot and warm rolling [9,10], hot extrusion with high reduction ratio [11,12] and a combination of extrusion and hot rolling [13] have been successfully used to refine coarse microstructure and consequently enhance mechanical properties of magnesium alloys. However, no research about the effect of hot rolling on Mg–Al–RE alloys has been reported. In present

* Corresponding author at: School of Materials and Chemical Engineering, Xi'an Technological University, Xi'an 710032, China.
Tel.: +86 29 83208080; fax: +86 29 83208080.
E-mail address: wjl810325@163.com (J. Wang).

0925-8388/$ – see front matter © 2010 Elsevier B.V. All rights reserved.
doi:10.1016/j.jallcom.2010.07.149

Table 1
Chemical composition (wt.%) of Mg–5Al–0.3Mn–2Nd alloy.

Al	Nd	Mn	Mg
4.99	2.01	0.34	Balance

work, Mg–5Al–0.3Mn–2Nd alloy was prepared and hot-rolled. The microstructure and mechanical properties of the as-cast, hot-rolled and annealed samples were investigated.

2. Experimental procedures

Nominal composition of the studied alloy is Mg–5Al–0.3Mn–2Nd. Commercially pure Mg (99.5%) and high pure Al (99.9%) were used. Mn and Nd were added in form of Al–10 wt.% Mn and Mg–23 wt.% Nd master alloys. The studied alloy was melted and alloyed at 780 °C by using a mild steel crucible in an electric resistance furnace under the protection of a mixed gas atmosphere of SF_6 (1%, volume fraction) and CO_2 (Bal.). The melt was homogenized at 750 °C for 0.5 h, and then cast into a metal mould that was preheated to about 300 °C. The size of ingot is 200 mm × 100 mm × 20 mm. Chemical composition of the studied alloy was determined by inductively coupled plasma atomic emission spectroscopy (ICP-AES) and the results were listed in Table 1. The cast ingots were homogenized at 410 °C for 20 h followed by water quenching and then machined into 4 mm plate for rolling. Hot rolling was processed at 400 °C using a two-high rolling mill with 150 mm in roll diameter and 190 mm in roll width. During rolling process, no heating was conducted on the rolls and the roll speed is 2 m/min. Prior to rolling, specimen was preheated at 400 °C for 10 min in a furnace and then immediately rolled. Repetitive preheating was done in the furnace between passes to regain the given rolling temperature. The specimen was air cooled after final pass and a sheet with total thickness reduction of 63% was obtained through 5 passes with different thickness reduction per pass. After hot rolling, the rolled sheets were annealed at 250 °C with different time to investigate the microstructure evolution.

Microstructures of the as-cast, hot-rolled and annealed samples were characterized by optical microscope (OM, Olympus GX71) and scanning electron microscope (SEM, FEI XL-30 ESEM) equipped with an energy dispersive X-ray spectrometer (EDX, Oxford). Specimens for OM and SEM were prepared by standard technique of grinding and polishing, followed by etching with acetic–picric acid solution (5 mL CH_3COOH, 2.1 g picric acid, 5 mL water and 35 mL alcohol). Phase constitutions of the samples were analyzed by X-ray diffraction (XRD, D/Max 2500V PC). For the hot-rolled and annealed samples, XRD tests were conducted on the rolled planes both for phase analysis and texture investigation. Microhardness of the samples was conducted under a Vickers hardness (Hv) Tester (FM-700) with a loading force of 25 g and holding time of 15 s. The final hardness value was given as average of at least 6 measurements. Uniaxial tensile test was carried out on Instron-5869 testing machine at room temperature with an initial strain rate of $5.6 \times 10^{-4}\ s^{-1}$. Gauge sections of tensile specimens are 15 mm in length, 3.5 mm in width and 1.5 mm in thickness. Tensile specimens for hot-rolled and annealed samples were machined from hot-rolled sheet with the gauge-length lying parallel to the rolling direction. Ultimate tensile strength (UTS) is indicated by the maximum of a stress–strain curve. Yield strength is defined by the "0.2% offset strain". The yield strength at 0.2% offset is determined by finding the intersection of the stress–strain curve with a line parallel to the initial slope of the curve and which intercepts the abscissa at 0.2%. Elongation is the increase in the gauge-length of a test specimen after fracture divided by its original gauge-length, which is determined by manual measurement after tensile test. Strain is the ratio of deformation dimension to the original dimension. Values of UTS, YS and elongation are given as averages of 5 measurements. The fracture surfaces of the samples were also analyzed by SEM.

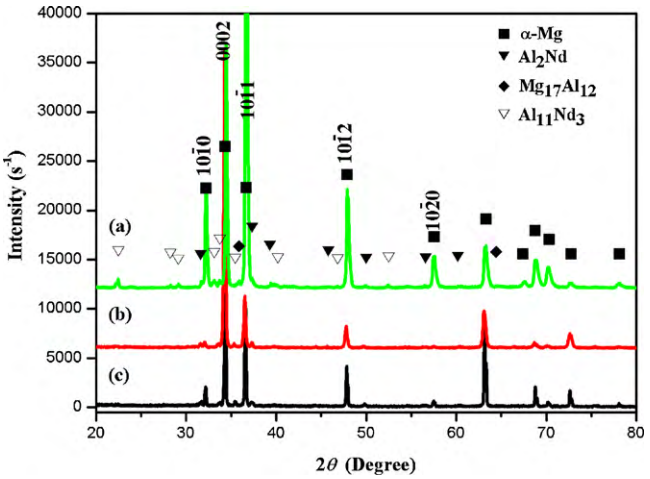

Fig. 1. XRD patterns of Mg–5Al–0.3Mn–2Nd alloy: (a) as-cast sample; (b) hot-rolled sample; (c) sample annealed at 250 °C for 40 min.

3. Results and discussion

3.1. XRD analysis

Fig. 1 shows XRD patterns of Mg–5Al–0.3Mn–2Nd alloy in different states. It can be seen that the as-cast sample is mainly composed of α-Mg, Al_2Nd, $Mg_{17}Al_{12}$ and $Al_{11}Nd_3$ phases. Phase compositions of the hot-rolled sample and the sample annealed at 250 °C for 40 min are almost the same. They both consist of α-Mg, Al_2Nd and $Al_{11}Nd_3$ phases, except for $Mg_{17}Al_{12}$. The disappearance of $Mg_{17}Al_{12}$ phase is due to homogenization of the studied alloy at 410 °C for 20 h. In addition, peaks intensities for α-Mg phase are different for the three state samples. Compared with those of the as-cast sample, intensities of {10$\bar{1}$0}, {10$\bar{1}$1}, {10$\bar{1}$2} and {10$\bar{2}$0} reflection for the hot-rolled sample decrease greatly, but the intensity of {0002} reflection increases obviously. This suggests that the hot-rolled sample exhibit a typically strong {0002} basal texture. Similar results were also reported in [14,15]. It can also be observed from Fig. 1 that the {0002} basal texture is weakened through annealing treatment as the intensity of {0002} reflection decreases compared with that of the hot-rolled sample.

3.2. Microstructure of the as-cast, hot-rolled and annealed samples

Grain structure of the as-cast sample is illustrated in Fig. 2(a). Equiaxed grains are observed and the average grain size is about 90 μm. Optical microstructure of the as-cast sample is demonstrated in Fig. 2(b). It is noted that the as-cast sample consists of

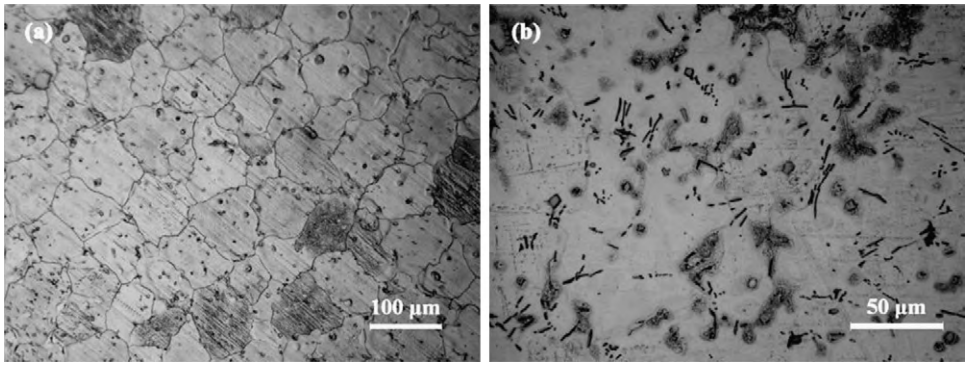

Fig. 2. Grain structure (a) and optical microstructure (b) of the as-cast sample.

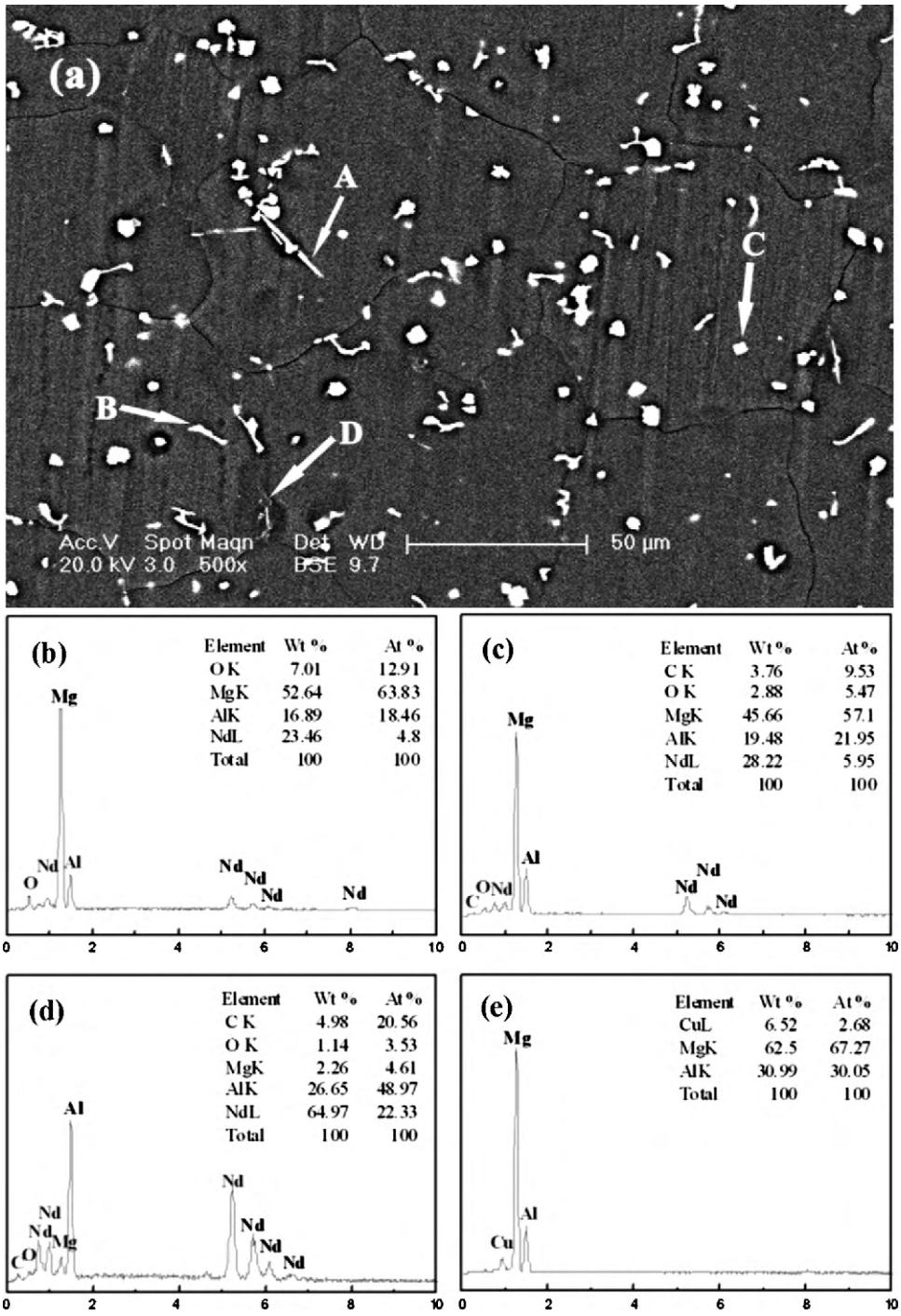

Fig. 3. SEM image and EDX analysis of the compounds in the as-cast sample: (a) SEM image, (b) EDX analysis of the compound A in (a); (c) EDX analysis of the compound B in (a); (d) EDX analysis of the compound C in (a); (e) EDX analysis of the compound D in (a).

long acicular precipitate, polygonal particles and island-like phase. These phases can also be observed in SEM image shown in Fig. 3(a), in which A and B are labeled for long acicular phase, C for polygonal particle and D for island phase, correspondingly. Their elemental compositions are examined by EDX and results are shown in Fig. 3(b)–(e). It is illustrated in Fig. 3(b) and (c) that the atomic ratios of Al:Nd for acicular phase A and B are 3.85 and 3.69, respectively. These two values are well in agreement with the stoichiometric ratio 11:3 (3.67). According to the result of XRD analysis, chemical formula of the acicular phase could be confirmed as $Al_{11}Nd_3$. For the polygonal particle labeled as C, EDX result shows that Al:Nd ratio is 2.19, which is near to 2:1. Based on the XRD results, the polygonal particle could be identified as Al_2Nd phase. While for the island-shaped phase labeled as D, EDX analysis reveals that it consists of Al and Mg elements. Combining the results of XRD analysis, it could be confirmed as $Mg_{17}Al_{12}$ phase. The Al_2Nd phase does not appear in our previous work [16], which might be attributed to different casting moulds that causes different solidification rates.

Fig. 4 demonstrates the SEM image of hot-rolled sample. It is noted that the microstructure and morphology of precipitates are all changed after hot rolling. Twins are clearly observed and they distribute throughout the sample. Grain boundaries become wavy and the average grain size decreases to about 20 μm as a result of dynamic recrystallization (DRX) during repeated preheating and

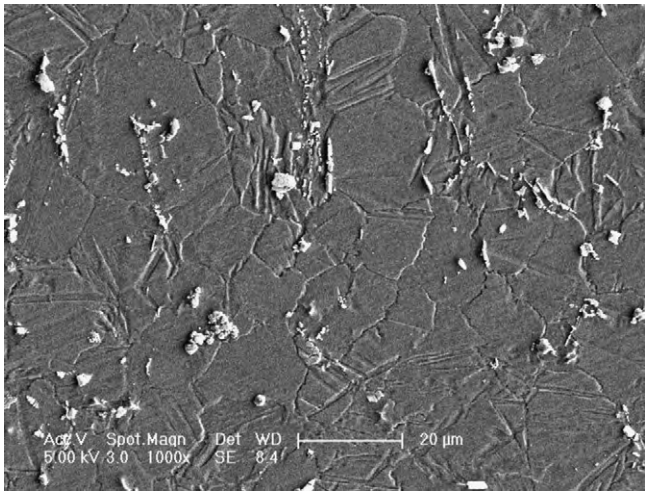

Fig. 4. SEM image of the hot-rolled sample.

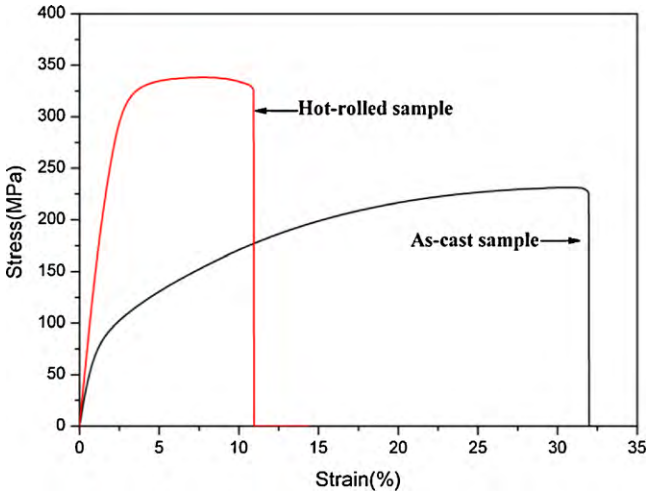

Fig. 6. Stress–strain curves for as-cast and hot-rolled samples of Mg–5Al–0.3Mn–2Nd alloy.

hot rolling. In addition, the acicular $Al_{11}Nd_3$ phases about 30 μm in length in the as-cast sample (as shown in Fig. 2) break into many small sections after hot rolling.

Annealing treatment was carried out to investigate microstructure evolutions of the hot-rolled sample. Fig. 5 demonstrates optical microstructure of the hot-rolled sample annealed at 250 °C for various time. Compared with the hot-rolled sample, it can be seen that twins disappear and the average grain size becomes much smaller in the sample annealed at 250 °C for 20 min. The average grain size is about 10 μm. This microstructure refinement implies that the annealed microstructure evolves by recrystallization rather than grain growth. With further increasing the annealing time, there is little variation for the average grain size, which indicates that the hot-rolled sample exhibits high thermal stability. It is because DRX-grain growth is restricted by the $Al_{11}Nd_3$ and Al_2Nd phases during annealing process.

3.3. Mechanical properties of the as-cast, hot-rolled and annealed samples

Mechanical properties of the as-cast and hot-rolled samples along rolling direction are tested at room temperature. Fig. 6 shows a set of typical stress–strain curves of the as-cast and hot-rolled samples. It is clearly seen that for the as-cast sample, strength increases with increasing strain after yielding. It is meant that the as-cast sample possesses a strong strain-hardening behavior. After hot rolling, strain-hardening phenomenon disappears and necking can be observed in Fig. 6 for the hot-rolled sample. Mechanical properties of the as-cast and hot-rolled samples are listed in Table 2. Vickers hardness, UTS and YS of the as-cast sample are about 52, 230 MPa and 65 MPa respectively. After hot rolling, Hv, UTS and YS are about 76, 340 MPa and 240 MPa. Compared with those of the

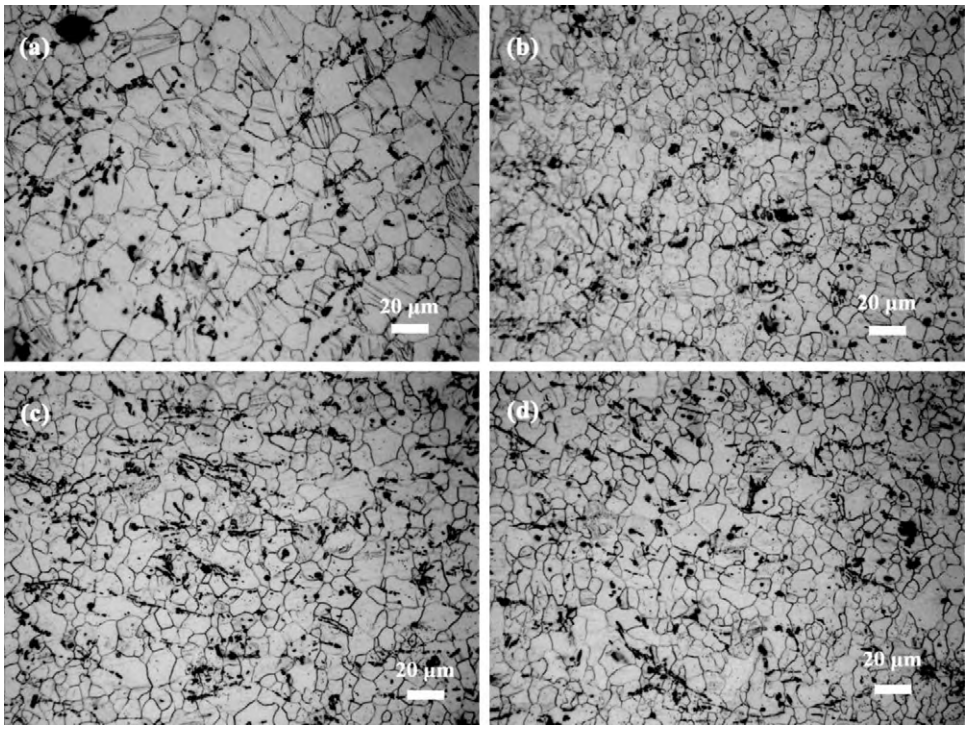

Fig. 5. Optical microstructures of hot-rolled sample annealed at 250 °C for different time: (a) 0 min; (b) 20 min; (c) 40 min and (d) 60 min.

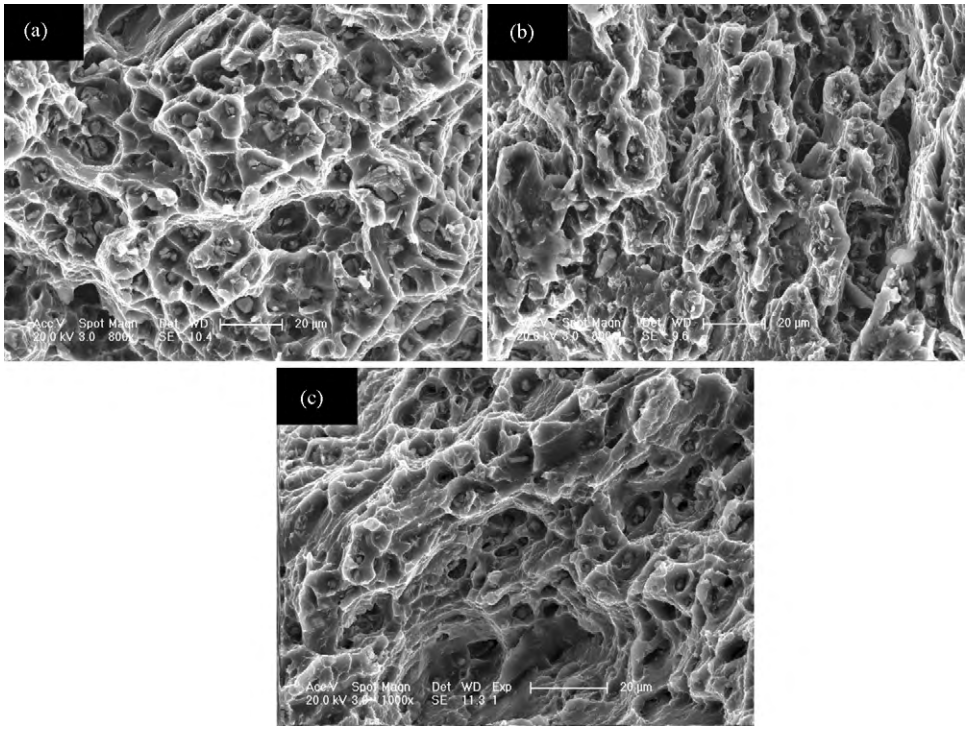

Fig. 7. SEM fractographs of Mg–5Al–0.3Mn–2Nd alloy: (a) as-cast sample; (b) hot-rolled sample; (c) sample annealed at 250 °C for 40 min.

as-cast sample, they are increased by 46%, 47.8% and 269%, correspondingly. However, elongation sharply decreases from 29% to 9%.

Mechanical properties of the hot-rolled samples annealed at 250 °C for 20 min, 40 min and 60 min are also tested. The related mechanical properties are summarized in Table 2 as well. It can be concluded from Table 2 that the Hv, UTS and YS of the annealed samples decrease a little compared with those of the hot-rolled sample, but they are still much higher than those of the as-cast sample. In addition, the elongation recovers to more than 24%, which is comparable to that of the as-cast sample. With increasing annealing time, little variation for the mechanical properties can be observed.

Compared the UTS and YS of the as-cast sample with those of the hot-rolled sample, it can be concluded that the UTS and YS are obviously enhanced through hot rolling. The improvement can be ascribed to following reasons. Firstly, grain size is obviously refined by hot rolling via DRX. Average grain size decreases from 90 μm for the as-cast sample to 20 μm for the hot-rolled sample. According to the Hall–Petch relationship, strength of the hot-rolled sample can be greatly enhanced through grain-refining effect. Secondly, after the hot-rolling process, the long acicular $Al_{11}Nd_3$ phase in the as-cast sample breaks into the many small sections in the hot-rolled sample. Their cutting effect on the matrix could be relieved. Consequently, crack initiation and propagation becomes much more difficult. Thirdly, as the density of $Al_{11}Nd_3$ particles becomes much larger, dislocation density is increased by hot rolling. Moreover, the cracked $Al_{11}Nd_3$ and Al_2Nd particles could strengthen the alloy greatly through interacting strongly with dislocations and pinning them during deformation process.

Table 2
Mechanical properties of the as-cast, hot-rolled and annealed samples at room temperature.

Samples	Hv	UTS (MPa)	YS (MPa)	Elongation (%)
As-cast	52	230	65	29
Hot-rolled (along the rolling direction)	76	340	240	9
Annealed 20 min	64	279	160	24
Annealed 40 min	63	270	157	25
Annealed 60 min	62	271	152	27

3.4. Fracture

The as-cast sample exhibits an elongation of about 29%. After hot rolling, it decreases to 9%. While for the annealed samples, elongation recovers to 24–27% again. These changes can also be indexed from the fracture surfaces of these samples. SEM fractographs of the as-cast sample, hot-rolled sample and sample annealed at 250 °C for 40 min are shown in Fig. 7. For the as-cast sample seen in Fig. 7(a), ductile dimples, cleavage facets and cracks can be clearly observed. This implies that the as-cast sample exhibits a quasi-cleavage fracture mode. As shown in Fig. 7(b), the hot-rolled sample takes an intergranular fracture mode and fails along the grain boundaries, which illustrates a brittle failure mode. These variations can be understood from two aspects. Firstly, the hot-rolled sample displays the strongest basal texture among three samples. Secondly, the internal stress and dislocation density in the hot-rolled sample becomes much higher compared with the as-cast sample. These two factors account for the brittleness of the hot-rolled sample. After annealing, the intensity of basal texture and the internal stress are significantly reduced and dislocations annihilation also happens. Therefore, the alloy becomes ductile again with elongation about 24–27%. This can be confirmed form the SEM fractograph of the sample annealed at 250 °C for 40 min. In Fig. 7(c), ductile dimples appears again, indicating that this sample take a more ductile failure mode.

4. Conclusions

Microstructure and mechanical properties of the as-cast, hot-rolled and annealed samples of the Mg–5Al–0.3Mn–2Nd alloy were investigated. The following conclusions can be drawn:

(1) Average grain size of the as-cast sample is about 90 μm. Through dynamic recrystallization, it is greatly refined to about 20 μm for the hot-rolled sample. The long acicular $Al_{11}Nd_3$ phase also breaks into many small sections after hot rolling.
(2) The ultimate tensile strength (UTS) and yield strength (YS) of the hot-rolled sample are about 340 MPa and 240 MPa respectively. Compared with those of the as-cast sample, they are enhanced by 47.8% and 269% correspondingly.
(3) The improvement of the UTS and YS of the hot-rolled sample is ascribed to the grain-refining strengthening and relieving of the cutting effect of the $Al_{11}Nd_3$ phase. The cracked $Al_{11}Nd_3$ phase and Al_2Nd particles can also strengthen the alloy by strongly interacting with dislocations and pinning them.
(4) The average grain size becomes even smaller for the hot-rolled sample annealed at 250 °C for 20 min. With increasing the annealing time, no obvious grain-coarsen is observed and there is little variation for the mechanical properties, which indicates that the hot-rolled sample exhibits very high thermal stability.

Acknowledgements

This work is financially supported by CAS for Distinguished Talents Program, The Science Program of the Promotes Northeast of CAS (KGCX2-SW-216) and Science and Technology Program of Changchun (08YJ09). The authors would like to express their thanks to Dr. Jie Yang for beneficial discussions. The authors would also appreciate Miss Guihua Su for experimental assistance.

References

[1] I.P. Moreno, T.K. Nandy, J.W. Jones, J.E. Allison, T.M. Pollock, Scripta Mater. 45 (2001) 1423–1429.
[2] I.P. Moreno, T.K. Nandy, J.W. Jones, J.E. Allison, T.M. Pollock, Scripta Mater. 48 (2003) 1029–1034.
[3] J. Bai, Y.S. Sun, S. Xun, F. Xue, T.B. Zhu, Mater. Sci. Eng. A 419 (2006) 181–188.
[4] T. Kr. Anne, H. Westengen, Proceedings of the International Conference on Magnesium Alloys and their Applications, Garmisch-Partenkirchen, FRG, 1992, pp. 221–228.
[5] P. Bakke, H. Westengen, in: P.A. Warrendale (Ed.), Proceedings of Magnesium Technology, TMS, 2005, pp. 291–296.
[6] Callister W.D.Jr., Fundamentals of Materials Science and Engineering, fifth ed., Chemical Industry Press, Beijing, 2002, p. 207.
[7] R. Armstrong, I. Codd, R.M. Douthwaite, N.J. Petch, Philos. Mag. 7 (1962) 45–58.
[8] Y.C. Lee, A.K. Dahle, D.H. StJohn, Metall. Mater. Trans. A 31 (2000) 2895–2906.
[9] T. Mohri, M. Mabuchi, M. Nakamura, T. Asahina, H. Iwasaki, T. Aizawa, K. Higashi, Mater. Sci. Eng. A 290 (2000) 139–144.
[10] T.C. Chang, J.Y. Wang, C.M. O, S. Lee, J. Mater. Proc. Technol. 140 (2003) 588–591.
[11] T. Mohri, M. Mabuchi, N. Saito, M. Nakamura, Mater. Sci. Eng. A 257 (1998) 287–294.
[12] A. Bussiba, A. Ben Artzy, A. Shtechman, S. Ifergan, M. Kupiec, Mater. Sci. Eng. A 302 (2001) 56–62.
[13] A. El-morsy, A. Ismail, M. Waly, Mater. Sci. Eng. A 486 (2008) 528–533.
[14] S.H. Kim, B.S. You, C.D. Kim, Y.M. Seo, Mater. Lett. 59 (2005) 3876–3880.
[15] B.P. Zhang, Y.F. Tu, J.Y. Chen, H.L. Zhang, Y.L. Kang, H.G. Suziki, J. Mater. Proc. Technol. 184 (2007) 102–107.
[16] J.L. Wang, J. Yang, Y.M. Wu, H.J. Zhang, L.M. Wang, Mater. Sci. Eng. A 472 (2008) 332–337.